Electronic Supplementary Material (ESI) for Sensors & Diagnostics.

Electronic Supplementary Information (ESI)

S1 Parts of the device

The materials chosen are in accordance with that are used in commercially available kits for lateral flow assays. For the model, the composition of the test membrane was selected to be nitrocellulose fiber FF120HP. The sample pad and conjugate pad were made up of cellulose fibers CF3, while the wicking pad was composed of cellulose fibers CFSP. The thickness of different materials is considered as 125 μm for nitrocellulose, 1000 μm for cellulose fibers [1–3]. The material properties for each of the section is defined while simulating the Richards' equation interface in COMSOL.

Table S1 Different parts of the lateral flow assay

Sl. No.	Part of the device	Paper material	Thickness of the material (in μm)	Van-Genuchten parameters		
				$\frac{1}{\alpha\, m}$	n	l
1	Sample and conjugate pads	Cellulose fibers (CF3)	900	4.3	1.41	0.5
2	Working membrane	Nitrocellulose fibers (FF120HP)	100	1	2.33	0.5
3	Wicking pad	Cellulose fibers (CFSP)	1000	4.3	1.41	0.5

For the geometry, we considered three possible cases; (i) a 2D model with uniform thickness, (ii) 2D model considering the thickness variations, and (iii) 2D model with thickness variation and the presence of overlaps between the different domains. We modelled our system relaxing the assumptions of thickness of the materials and overlaps between different parts of the materials, sequentially, and obtained the velocity profiles. We observed that the fluid fronts for our model is almost on same position for same time values as that of a modified geometry with overlap for both 2D and 3D models. This signifies validation in the value of velocity of sample at distinct instances. Moreover, the little changes in velocities at overlaps because of geometric variations are clearly visible with the help of heat maps. Fig. S1 depicts the velocity profiles for different geometries. Since the model with varying thickness (Table S1) as well as with the presence of overlaps is the closest possible one resembling commercially available LFIA devices, we considered this geometry for further simulations.

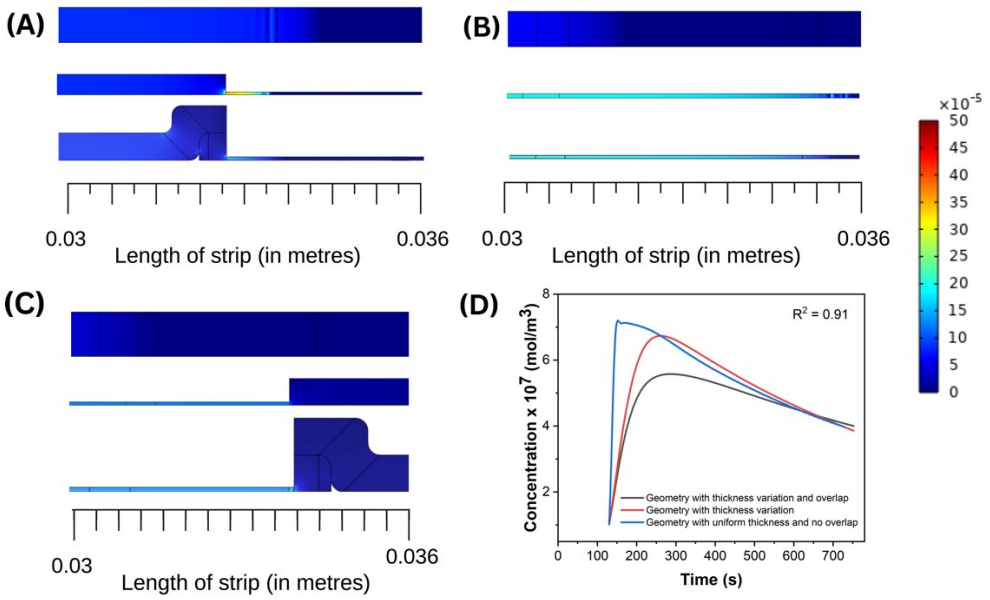

Fig. S1 Velocity plots for previous geometry in comparison with modified geometries that consider the thickness variation and overlap of the paper materials in the nitrocellulose working membrane at (A) 35 seconds (B) 65 seconds (C) 105 seconds ; (D) Profiles of analyte concentrations for different geometries.

S2 Relevant initial and boundary conditions

The following initial and boundary conditions were used to solve eqn (6): the initial concentration of competitor molecules on test line is 5x10^{-6} $\frac{mol}{m^2}$ ($C\_in \times T\_s$), and that of the secondary antibodies on control line is 5x10^{-6} $\frac{mol}{m^2}$ ($Q\_in \times T\_s$), the inflow concentration of A (A_in) and P (P_in) is 1×10^{-6} to $5 \times 10^{-4} \frac{mol}{m^3}$ and $5 \times 10^{-5} \frac{mol}{m^3}$ respectively. Additionally, at the outlet, an outflow condition ($-n.\nabla C_i = 0$) was maintained. For solving eqn (8), the initial saturation over the entire domain was as assumed to be zero, whereas the saturation at the inlet boundary was at its maximum (θ_s), and no-flow condition was maintained at all other boundaries of the domain. The initial pressure head over the whole device is –5.3 m, and over sample pad a boundary condition of pressure (p0 = -0.002 pa) is maintained. The inlet, outlet and other boundary conditions are presented schematically in Fig. S2.

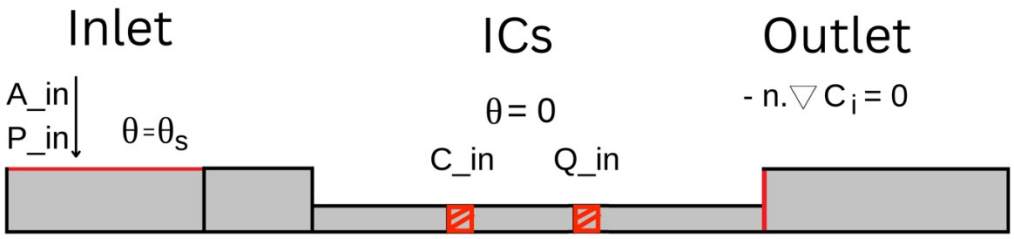

Fig. S2 Schematic showing the inlet, outlet and other boundary conditions along with the initial conditions (ICs) in the LFIA. Except the inlet and outlet, all other boundaries are fixed to "No-slip" boundary condition.

S3 Genesis & Definition of non-dimensional numbers

Considering species-transport equation, mentioned in section 2.1,

$$\frac{\partial}{\partial t}Ci = Di \times \left(\frac{\partial}{\partial x^2}Ci\right) - v \times \left(\frac{\partial}{\partial x}Ci\right) - ri \quad \text{(S1)}$$

$$where, ri = kCi^2$$

Non-dimensionalizing the above equation with appropriate constants, as mentioned below.

$C = \frac{Ci}{C_0}$

$\Gamma = \frac{t}{t_0}$

$\chi = \frac{x}{L}$

$v = \frac{v}{v_0}$

Substituting the above in eqn (S1) gives non-dimensional species-transport equation,

$$\frac{C_0}{t_0}\left(\frac{\partial}{\partial \Gamma}C\right) = Di \times \left(\frac{C_0}{L^2}\right) \times \left(\frac{\partial}{\partial \chi^2}C\right) - \left(\frac{v_0 \cdot C_0}{L}\right) \times v \times \left(\frac{\partial}{\partial \chi}C\right) - \left(kC_0{}^2\right) \times C^2 \quad \text{(S2)}$$

Dividing eqn (2) with $\left(\frac{v_0 \cdot C_0}{L}\right)$,

$$\left(\frac{L}{v_0 \cdot t_0}\right) \times \left(\frac{\partial}{\partial \Gamma}C\right) = \left(\frac{Di}{v_0 \cdot L}\right) \times \left(\frac{\partial}{\partial \chi^2}C\right) - v \times \left(\frac{\partial}{\partial \chi}C\right) - \left(\frac{k \cdot C_0 \cdot L}{v_0}\right) \times C^2 \quad \text{(S3)}$$

From eqn (S3), it can be observed that

$\left(\frac{v_0 \cdot L}{Di}\right)$ is a non-dimensional number which compares extent of diffusion and convection for transport of a fluid in a medium, specifically known as Peclet number.

Peclet numbers (*Pe*) account for flow through channels by comparing the convection and diffusion components of the flow. The dominant component and its influence on the flow may be precisely recognised by calculating *Pe*. The Peclet number is defined below as a comparison of the time scales of convection and diffusion.[4]

The diffusive time scale for species to diffuse a length 'l' is $\left(\frac{l^2}{D}\right)$; the convective time scale for species to travel a length 'l' is $\left(\frac{l}{u}\right)$; and the velocity utilised in the convective time scale is derived from Richard's equation. *Pe* = (Diffusive time scale / Convective time scale). Mathematically,

$$Pe = \left(\frac{\left(\frac{l^2}{D}\right)}{\left(\frac{l}{u}\right)}\right)$$

$$Pe = \frac{(u \cdot l)}{D} \quad \text{(S4)}$$

Where u is the velocity of the sample.

l is the characteristic length.

D is the diffusion coefficient of the sample.

In this study, Peclet number was calculated across the timeline when the sample resides in the working membrane with velocity spatially averaged over the working membrane. The calculation of *Pe* for certain values in the timeline are provided in Table S2.

Table S2 Calculation of *Pe* for certain time points

S.No.	Time (t in seconds)	U [m/s]	$\frac{D\left[\frac{m^2}{s}\right]}{l[m]}$	***Pe***
1	100	6.89×10^{-5}	1.82×10^{-9}	3.78×10^{4}
2	110	7.02×10^{-5}	1.82×10^{-9}	3.85×10^{4}
3	120	7.11×10^{-5}	1.82×10^{-9}	3.9×10^{4}
4	130	7.16×10^{-5}	1.82×10^{-9}	3.93×10^{4}
5	140	7.19×10^{-5}	1.82×10^{-9}	3.95×10^{4}
6	150	7.2×10^{-5}	1.82×10^{-9}	3.96×10^{4}
7	160	7.19×10^{-5}	1.82×10^{-9}	3.95×10^{4}
8	170	7.18×10^{-5}	1.82×10^{-9}	3.94×10^{4}
9	180	7.19×10^{-5}	1.82×10^{-9}	3.95×10^{4}
10	190	7.2×10^{-5}	1.82×10^{-9}	3.96×10^{4}
11	200	7.18×10^{-5}	1.82×10^{-9}	3.94×10^{4}
12	210	7.09×10^{-5}	1.82×10^{-9}	3.89×10^{4}
13	220	6.91×10^{-5}	1.82×10^{-9}	3.8×10^{4}
14	230	6.65×10^{-5}	1.82×10^{-9}	3.65×10^{4}
25	240	6.31×10^{-5}	1.82×10^{-9}	3.47×10^{4}
16	250	5.9×10^{-5}	1.82×10^{-9}	3.24×10^{4}
17	260	5.4×10^{-5}	1.82×10^{-9}	2.97×10^{4}
18	270	4.82×10^{-5}	1.82×10^{-9}	2.65×10^{4}
19	280	4.19×10^{-5}	1.82×10^{-9}	2.3×10^{4}
20	290	3.54×10^{-5}	1.82×10^{-9}	1.94×10^{4}
21	300	2.93×10^{-5}	1.82×10^{-9}	1.6×10^{4}

Similarly, $\left(\frac{k \cdot C_0 \cdot L}{v_0}\right)$ = *Da* from eqn (S3) is a non-dimensional number which compares the extent of reaction to transport for a species getting transported in a reacting medium. Damköhler number accounts for the kinetics and transport in the LFIA device by comparing flow and reaction. *Da* indicates which component is more responsible for altering the signal on the test and control lines on the working membrane. *Da can be* further approximated with the dominating parameter affecting the overall rates. Damköhler number can be expressed as follows:[5]

$$Da = \left(\frac{\left(\frac{l}{u}\right)}{\left(\frac{P}{Rt}\right)}\right) \quad \text{(S5)}$$

$$Rt = \left(K_{on} . P . C - K_{off} . PC\right) \quad \text{(S6)}$$

Where K_{on} is the forward reaction rate constant for the reaction on test line. P, C are concentrations of reporter and competitor molecules respectively. u is the velocity of sample. l is the characteristic length. Rt is the rate of surface reaction on test line.

The velocity of the sample is obtained from Richard's equation, and the convective time scale related to flow is (l/u). The reaction time is proportional to the concentration of limiting species in the reaction, P (as shown in Table. S1), and the pace of the reaction.

$$Da = \frac{K_{on} . P . C - K_{off} . PC}{\frac{u}{l} . (P)} \quad \text{(S7)}$$

For the kinetics under the current study, $K_{off} . PC$ <<< $K_{on} . P . C$;
So, we can approximate *Da* as :

$$Da = \frac{K_{on} . C}{\frac{u}{l}} \quad \text{(S8)}$$

S4 Signal Intensity (T/C) obtained for Sandwich Immunoassay:

The architect of the Lateral Flow Immunoassay (LFIA) device operating in sandwich format is similar to the one reported in Fig. 1, containing a sample pad, conjugate pad, test line, and control line. The target analyte (A) is introduced on sample pad, then the sample flows to conjugate pad, where reporter particles (primary antibodies conjugated with sensing elements) are placed. Further, the sample enters working membrane, which contains test and control line. Primary antibodies (R) and secondary antibodies (Q) are pre-concentrated on the test and control lines, respectively. Finally, it flow pasts working membrane and reaches wicking pad. The bulk and surface reactions take place on the LFIA operating in sandwich format are,

Bulk Reaction:

$$A + P \leftrightarrow AP \quad \text{(S9)}$$

Surface Reactions (Test line):

$$R + A \leftrightarrow RA \quad \text{(S10)}$$
$$AP + R \leftrightarrow RPA \quad \text{(S11)}$$
$$RA + P \leftrightarrow RPA \quad \text{(S12)}$$

Surface Reactions (Control line):

$$P + Q \leftrightarrow PQ \quad \text{(S13)}$$
$$AP + Q \leftrightarrow APQ \quad \text{(S14)}$$
$$A + PQ \leftrightarrow APQ \quad \text{(S15)}$$

RPA is the signal forming compound at test line, and it APQ + PQ for control line. T/C was shown to rise monotonically at low analyte concentrations (Fig. 4A). This occurs because the signal at the control line (PQ + APQ) saturates rapidly due to the abundance of unbound reporter particles. A low analyte concentration suggests a low concentration of AP formed, whereas the signal at the test line saturates gradually. Consequently, the test line signal increases as the control line becomes saturated after a while. Thus, an increasing trend in T/C with time at low concentrations can be observed. The T/C value increases, then declines, and finally approaches saturation at moderate analyte concentrations (Fig. 4B). This observation is relevant to the dominance of the hook effect only after a particular analyte concentration is attained. T/C, on the other hand,

declines monotonically with time when the concentration on the test line reaches saturation owing to the availability of more unbound analytes to the control line, as illustrated in Fig. 4C. Because the hook effect is considerable in this case, the test line signal is low when compared to low and moderate analyte concentrations.

The test line signal i.e. concentration of RPA increases as the concentration of A increases to a certain level. Further, with the increase in concentration of A, the free A reaching test line increases, so the reaction. S10 proceeds faster in the forwarding direction (according to Le chart liar's principle), so the concentration of RA increases. As more free A reaches and is bound with R in the test line, AP binding with R on the test line crossing the hinderic resistance of A particles bound there becomes difficult. So, the probability of reaction. S11 goes down. And as the concentration of RA increases reaction. S12 proceeds fast in the forward direction and the concentration of RPA starts increasing (according to Le chart liar's principle). As the concentration of RPA increases, reaction. S11 proceeds backward, according to Le chart liar's principle, and reaction. S12 will still proceed forward because the concentration of RA is increasing. So, in all these effects after a threshold concentration of A (analyte) the test line signal(concentration of RPA) goes down, this effect is called the Hook effect. For further detailed understanding on hook effect, the readers can refer to the text elsewhere.[6]

S5 Control line concentration vs time plot for sandwich immunoassay:

Fig. S3 depicts the variation of concentration of the control line with time for the sandwich assay described in section 3.1. As observed, the concentration of APQ and PQ formed in the control line can does not vary much with respect to the analyte concentration. This signifies the fact that hook effect observed in case of sandwich assay is mainly contributed because of the signal at the test line.

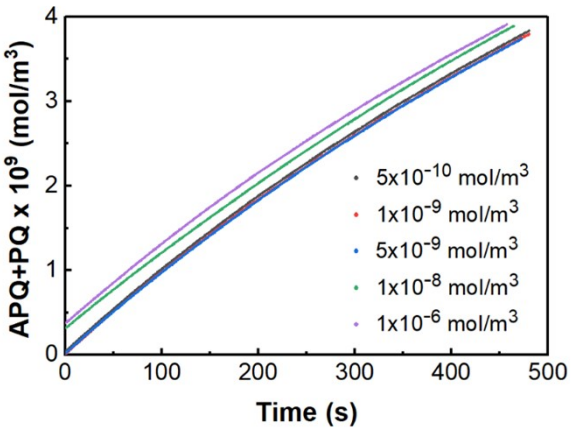

Fig. S3 Concentration of APQ+PQ on control line vs time for wide range of antigen concentration for Sandwich LFIA.

S7 Test line, and Control line concentration vs time plot for competitive immunoassay:

Fig. S4 depicts the variation of concentration of the test line and control line with time for the competitive assay described in section 3.3. As shown in Fig. S4A, concentration of PC, i.e., the signal formed on the test line, is inversely related to analyte concentration introduced on the sample pad. Fig. S4B shows that the concentration on the control lines doesn't vary much with change in inlet analyte concentration. Hence, in Fig. 7B, the trend of T/C with respect to analyte concentration signifies the trend of concentration of PC on the test line.

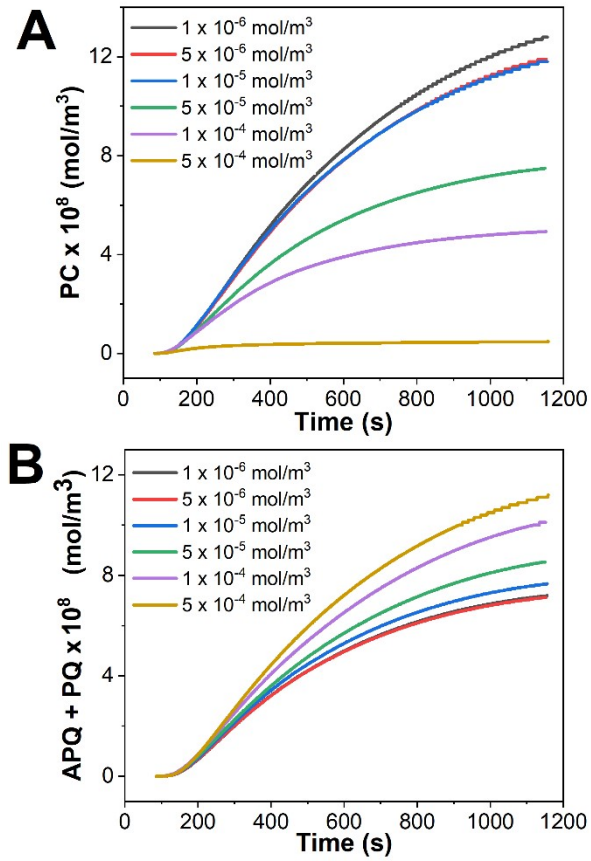

Fig. S4 A. Concentration of PC on test line vs time, B. Concentration of APQ+PQ on control line vs time for wide range of antigen concentration for Competitive LFIA.

S8 Signal intensity with respect to the forward kinetic constant

A trend similar to change in concentration of competitor molecules is observed here in Fig. S5. The occurrence of backward reaction is triggered after a certain value of forward reaction rate constant i.e., 10 (m^3/mol.s), decreases the T/C value. Hence it was concluded that this particular set of parameters to design the competitive LFIA, 10 (m^3/mol.s) is the optimum value of the forward rate constant.

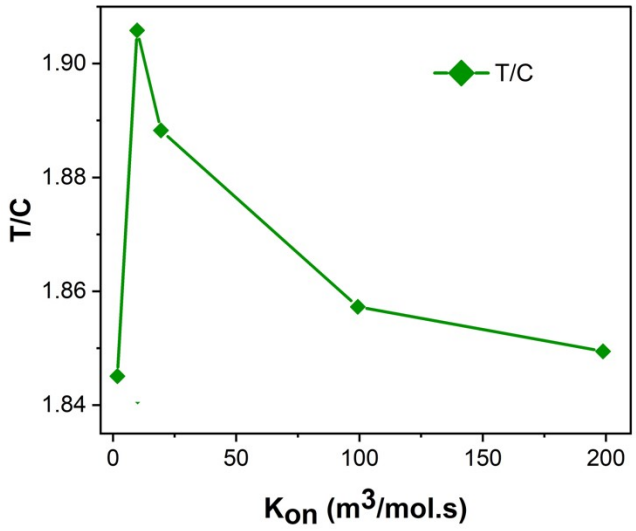

Fig. S5 T/C vs forward reaction rate constant for a competitive LFIA (saturated T/C values are considered i.e., time= 600 seconds). (For analyte concentration Ain = 1 x10^{-6} $\frac{mol}{m^3}$)

References:

1 Whatman FF120HP Membranes | Cytiva, https://www.cytivalifesciences.com/en/us/shop/whatman-laboratory-filtration/whatman-dx-components/lateral-flow-membranes/ff120hp-membranes-p-00760, (accessed March 1, 2023).

2 Whatman CF3 dipstick pad and papers | Cytiva, https://www.cytivalifesciences.com/en/us/shop/whatman-laboratory-filtration/whatman-dx-components/dipstick-pads-and-membranes/cf3-p-00757, (accessed March 1, 2023).

3 CFSP 20 cm x 30 cm sheet Lateral Flow, Assay Development, lateral flow immunoassays, lateral flow assay device, Immunoassay IVDs | Sigma-Aldrich, https://www.sigmaaldrich.com/IN/en/product/mm/cfsp22305pk, (accessed March 1, 2023).

4 B. E. Rapp, in *Microfluidics: Modelling, Mechanics and Mathematics*, Elsevier, 2017, pp. 243–263.

5 F. Yu and A. G. Hunt, *ACS Earth Space Chem*, 2017, **1**, 30–38.

6 S. Dodig, *Biochem Med (Zagreb)*, 2009, 50–62.